2023 American Control Conference (ACC)
San Diego, CA, USA. May 31 - June 2, 2023

Random-Walk Elimination in Numerical Integration of Sensor Data Using Adaptive Input Estimation

Sneha Sanjeevini and Dennis S. Bernstein

***Abstract*— Numerical integration of measured signals is challenging due to sensor noise, where sensor bias leads to a spurious ramp, and white noise leads to random-walk divergence. This paper presents a novel approach to numerical integration of sensor data based on adaptive input estimation. In particular, retrospective cost input estimation (RCIE) is applied to a one-step-delayed differentiator model to estimate the unknown input, which is the desired integral of the output. Numerical examples show that, for harmonic signals corrupted by white noise, RCIE integration eliminates the random walk that arises from standard numerical integration.**

I. INTRODUCTION

Integration is among the most fundamental operations in mathematics [1]. In applications, numerical integration methods are needed to compute integrals of functions as well as solutions to differential equations [2]–[4]. The present paper is concerned with numerical integration of signals given by sensor data, that is, measurements. Numerical integration of data is challenging due to the fact that sensor data are corrupted by noise. Measurement noise typically includes an unknown bias due to inexact sensor calibration [5] as well as random noise. Integration of the unknown bias leads to a ramp, while integration of the random noise leads to a random walk; both types of noise cause spurious divergence.

Integration of sensor data is of enormous importance in practice. In particular, for vehicle guidance and navigation, inertial navigation using strapdown sensors requires single integration of rate-gyro data to determine the vehicle attitude, while inertial navigation using either strapdown sensors or an inertially stabilized platform requires double integration of accelerometer data to determine the vehicle position [6]–[14].

Because of the importance of inertial navigation and related applications, researchers have developed techniques for mitigating spurious divergence and enhancing the accuracy of numerical integration of sensor data. In particular, [15], [16] developed a calibration technique for reducing the effect of sensor noise. In [17], the accuracy of trapezoidal and Romberg integration are compared for computing velocity in strapdown inertial navigation. In [18], bias removal and high-pass filtering techniques are used to remove drift. In [19], various methods are used to reduce drift. Likewise, in [20], stable variations of trapezoidal and Simpson integration methods are used to reduce drift. Finally, the accuracy of various numerical integration methods for inertial navigation is assessed in [17]–[20].

The present paper develops a novel approach to numerical integration of sensor data based on adaptive input estimation. In input estimation, the input to the system is assumed to be unknown, and the measured output of the system is used to estimate the input of the system. Non-adaptive input estimation is considered in [21]–[33], and adaptive input-estimation methods are considered in [34]–[39].

Among many potential applications, input estimation has been used for numerical differentiation. In particular, retrospective cost input estimation (RCIE) was used in [39] to estimate acceleration from position sensor data. To perform numerical differentiation, RCIE views the measurement as the integral of the input, and thus the estimated input approximates the derivative of the measurement. The accuracy of this technique is compared to alternative methods for numerical differentiation in [40]. A theoretical analysis of RCIE is given in [41].

The present paper applies RCIE to numerical integration. This is done by viewing the measurement as the derivative of the input so that the estimated input approximates the integral of the measurement. The differentiation dynamics used for this purpose are chosen to be a one-step-delayed model of the inverse of trapezoidal-integrator dynamics. This method is then applied to harmonic signals corrupted by white noise. In particular, RCIE is compared to numerical integration of the sensor data based on direct trapezoidal integration. It is shown that direct trapezoidal integration exhibits random-walk divergence, whereas RCIE integration eliminates the random walk. These effects are demonstrated for harmonic and dual-harmonic signals at different frequencies over a range of signal-to-noise ratios.

Section II summarizes the RCIE algorithm. Section III explains how RCIE is used for numerical integration. Numerical examples are illustrated in Section IV and the performance of RCIE is compared with trapezoidal integration. Section V concludes the paper.

II. RETROSPECTIVE COST INPUT ESTIMATION

Retrospective cost input estimation (RCIE) [39], [41] can be applied to MIMO linear time-varying systems. The objective in this paper is to use RCIE for integration, and for the purpose of integration, it is enough to consider SISO linear-time invariant systems. The RCIE algorithm presented here is specialized for the purpose of integration.

The authors are with the Department of Aerospace Engineering, University of Michigan, Ann Arbor, MI 48109, USA snehasnj@umich.edu, dsbaero@umich.edu

979-8-3503-2807-3/$31.00 ©2023 AACC

Consider the linear discrete-time system

$$x_{k+1} = Ax_k + Bd_k, \tag{1}$$
$$y_k = Cx_k + v_k, \tag{2}$$

where k is step, $x_k \in \mathbb{R}^{l_x}$ is the unknown state, $d_k \triangleq d(kT_\mathrm{s}) \in \mathbb{R}$ is a sample of the unknown input $d(t)$ at $t = kT_\mathrm{s}$, $y_k \triangleq y(kT_\mathrm{s}) \in \mathbb{R}$ is a measurement of the continuous-time signal $y(t)$ at $t = kT_\mathrm{s}$, and $v_k \in \mathbb{R}$ is zero-mean white Gaussian measurement noise with variance V_2. The matrices $A \in \mathbb{R}^{l_x \times l_x}$, $B \in \mathbb{R}^{l_x \times 1}$, and $C \in \mathbb{R}^{1 \times l_x}$ are assumed to be known. The goal is to estimate d_k and x_k.

RCIE consists of three subsystems, namely, the Kalman filter forecast subsystem, the input-estimation subsystem, and the Kalman filter data-assimilation subsystem. First, consider the Kalman filter forecast steps

$$x_{\mathrm{fc},k+1} = Ax_{\mathrm{da},k} + B\hat{d}_k, \tag{3}$$
$$y_{\mathrm{fc},k} = Cx_{\mathrm{fc},k}, \tag{4}$$
$$z_k = y_{\mathrm{fc},k} - y_k, \tag{5}$$

where $\hat{d}_k$ is the estimate of d_k, $x_{\mathrm{da,k}} \in \mathbb{R}^{l_x}$ is the data-assimilation state, $x_{\mathrm{fc},k} \in \mathbb{R}^{l_x}$ is the forecast state, $z_k \in \mathbb{R}$ is the innovations, and $x_{\mathrm{fc},0} = 0$. Next, to obtain $\hat{d}_k$, the input-estimation subsystem of order n_e is given by the exactly proper dynamics

$$\hat{d}_k = \sum_{i=1}^{n_\mathrm{e}} P_{i,k}\hat{d}_{k-i} + \sum_{i=0}^{n_\mathrm{e}} Q_{i,k} z_{k-i} + S_k, \tag{6}$$

where $P_{i,k} \in \mathbb{R}$ and $Q_{i,k} \in \mathbb{R}$ are output and input coefficients, respectively, and $S_k \in \mathbb{R}$ is a bias input. RCIE minimizes z_k by updating $P_{i,k}$, $Q_{i,k}$, and S_k. The subsystem (6) can be reformulated as

$$\hat{d}_k = \Phi_k \theta_k, \tag{7}$$

where the regressor matrix Φ_k is defined by

$$\Phi_k \triangleq \begin{bmatrix} \hat{d}_{k-1} & \cdots & \hat{d}_{k-n_\mathrm{c}} & z_k & \cdots & z_{k-n_\mathrm{c}} & 1 \end{bmatrix} \in \mathbb{R}^{1 \times l_\theta}, \tag{8}$$

the coefficient vector θ_k is defined by

$$\theta_k \triangleq \begin{bmatrix} P_{1,k} & \cdots & P_{n_\mathrm{c},k} & Q_{0,k} & \cdots & Q_{n_\mathrm{c},k} & S_k \end{bmatrix}^\mathrm{T} \in \mathbb{R}^{l_\theta}, \tag{9}$$

and $l_\theta \triangleq 2n_\mathrm{c} + 2$. In terms of the backward-shift operator $\mathbf{q}^{-1}$, (6) can be written as

$$\hat{d}_k = G_{\hat{d}z,k}(\mathbf{q}^{-1}) z_k + S_k, \tag{10}$$

where

$$G_{\hat{d}z,k} \triangleq D_{\hat{d}z,k}^{-1} N_{\hat{d}z,k}, \tag{11}$$
$$D_{\hat{d}z,k}(\mathbf{q}^{-1}) \triangleq I_{l_d} - P_{1,k}\mathbf{q}^{-1} - \cdots - P_{n_\mathrm{e},k}\mathbf{q}^{-n_\mathrm{e}}, \tag{12}$$
$$N_{\hat{d}z,k}(\mathbf{q}^{-1}) \triangleq Q_{0,k} + Q_{1,k}\mathbf{q}^{-1} + \cdots + Q_{n_\mathrm{e},k}\mathbf{q}^{-n_\mathrm{e}}. \tag{13}$$

To update the coefficient vector θ_k, define the filtered signals

$$\Phi_{\mathrm{f},k} \triangleq G_{\mathrm{f},k}(\mathbf{q}^{-1})\Phi_k, \quad \hat{d}_{\mathrm{f},k} \triangleq G_{\mathrm{f},k}(\mathbf{q}^{-1})\hat{d}_k, \tag{14}$$

where, for all $k \geq 0$, $G_{\mathrm{f},k}$ is a finite impulse response filter of order n_f given by

$$G_{\mathrm{f},k}(\mathbf{q}^{-1}) = \sum_{i=1}^{n_\mathrm{f}} \mathbf{q}^{-i} H_{i,k}, \tag{15}$$

$$H_{i,k} \triangleq \begin{cases} CB, & k \geq i = 1, \\ C\overline{A}_{k-1} \cdots \overline{A}_{k-i+1} B, & k \geq i \geq 2, \\ 0, & i > k, \end{cases} \tag{16}$$

$\overline{A}_k \triangleq A(I + K_{\mathrm{da},k}C)$, and $K_{\mathrm{da},k} \in \mathbb{R}^{l_x}$ is the Kalman filter gain (given by (22)). Furthermore, define the *retrospective performance variable*

$$z_{\mathrm{rc},k}(\hat{\theta}) \triangleq z_k - \left(\hat{d}_{\mathrm{f},k} - \Phi_{\mathrm{f},k}\hat{\theta}\right), \tag{17}$$

where the coefficient vector $\hat{\theta} \in \mathbb{R}^{l_\theta}$ denotes a variable for optimization, and define the retrospective cost function

$$J_k(\hat{\theta}) \triangleq \sum_{i=0}^{k} z_{\mathrm{rc},i}^\mathrm{T}(\hat{\theta}) R_z z_{\mathrm{rc},i}(\hat{\theta}) + (\hat{\theta} - \theta_0)^\mathrm{T} R_\theta (\hat{\theta} - \theta_0), \tag{18}$$

where $R_z \in \mathbb{R}$ is positive and $R_\theta \in \mathbb{R}^{l_\theta \times l_\theta}$ is positive definite. Define $P_0 \triangleq R_\theta^{-1}$. Then, for all $k \geq 0$, the cumulative cost function $J_k(\hat{\theta})$ has the unique global minimizer θ_{k+1} obtained by the recursive least squares update

$$P_{k+1} = P_k - P_k \Phi_{\mathrm{f},k}^\mathrm{T} \Gamma_k \Phi_{\mathrm{f},k} P_k, \tag{19}$$
$$\theta_{k+1} = \theta_k - P_k \Phi_{\mathrm{f},k}^\mathrm{T} \Gamma_k (\widetilde{z}_k + \Phi_{\mathrm{f},k}\theta_k), \tag{20}$$

where

$$\Gamma_k \triangleq (R_z^{-1} + \Phi_{\mathrm{f},k} P_k \Phi_{\mathrm{f},k}^\mathrm{T})^{-1}, \quad \widetilde{z}_k \triangleq z_k - \hat{d}_{\mathrm{f},k}. \tag{21}$$

Using the updated coefficient vector θ_{k+1}, the estimated input at step $k+1$ is calculated by replacing k by $k+1$ in (7). We choose $\theta_0 = 0$, and thus $\hat{d}_0 = 0$.

In order to estimate the state x_k, $x_{\mathrm{fc},k}$ is used to obtain the estimate $x_{\mathrm{da},k}$ of x_k given by the Kalman filter data-assimilation steps

$$K_{\mathrm{da},k} = -P_{\mathrm{f},k} C^\mathrm{T} (C P_{\mathrm{f},k} C^\mathrm{T} + V_2)^{-1}, \tag{22}$$
$$P_{\mathrm{da},k} = (I + K_{\mathrm{da},k} C) P_{\mathrm{f},k}, \tag{23}$$
$$x_{\mathrm{da},k} = x_{\mathrm{fc},k} + K_{\mathrm{da},k} z_k, \tag{24}$$
$$P_{\mathrm{f},k+1} = A P_{\mathrm{da},k} A^\mathrm{T} + V_{1,k}, \tag{25}$$

where $P_{\mathrm{f},k} \in \mathbb{R}^{l_x \times l_x}$ is the forecast error covariance, $P_{\mathrm{da},k} \in \mathbb{R}^{l_x \times l_x}$ is the data-assimilation error covariance,

$$V_{1,k} \triangleq B \ \mathrm{var}\ (d_k - \hat{d}_k) B^\mathrm{T} \tag{26}$$
$$+ A \ \mathrm{cov}\ (x_k - x_{\mathrm{da},k}, d_k - \hat{d}_k) B^\mathrm{T} \tag{27}$$
$$+ B \ \mathrm{cov}\ (x_k - x_{\mathrm{da},k}, d_k - \hat{d}_k) A^\mathrm{T}, \tag{28}$$

and $P_{\mathrm{f},0} = 0$. In this paper, we treat $V_{1,k}$ as a constant design parameter V_1.

III. NUMERICAL INTEGRATION BASED ON RCIE

In this section, we develop a numerical integration technique based on RCIE. In order to use RCIE as an integrator, the system (1), (2) is chosen to represent the discrete-time equivalent of a differentiator. The measured continuous-time output $y(t)$ is thus the derivative of the unknown input $d(t)$, which implies that the unknown input $d(t)$ is the integral of the measured output $y(t)$. Hence, by applying RCIE, $\hat{d}_k$ provides an estimate of the integral of the output $y(t)$. The differentiator dynamics used in RCIE are chosen to be the delayed inverse dynamics of a trapezoidal integrator. The trapezoidal integrator has the form

$$G_{\rm si}({\rm z}) \triangleq \frac{T_{\rm s}}{2}\frac{{\rm z}+1}{{\rm z}-1}, \tag{29}$$

and thus the one-step-delayed differentiator is

$$G_{\rm sd}({\rm z}) \triangleq \frac{2}{T_{\rm s}}\frac{{\rm z}-1}{{\rm z}^2+{\rm z}}. \tag{30}$$

The delay ensures that the differentiator is strictly proper. By applying RCIE with the state space realization of (30) given by

$$A = \begin{bmatrix} 0 & 1 \\ 0 & -1 \end{bmatrix}, \quad B = \begin{bmatrix} 0 \\ 2/T_{\rm s} \end{bmatrix}, \quad C = \begin{bmatrix} -1 & 1 \end{bmatrix}, \tag{31}$$

we can obtain an estimate of the integral of y.

IV. NUMERICAL EXAMPLES

In this section, numerical examples are presented to evaluate the accuracy of RCIE integration for sampled harmonic signals corrupted by noise. The performance of RCIE is compared with trapezoidal integration. The exact integral given by calculus is used as a baseline for comparison. The integral estimated by RCIE has a bias error on the order of 10^{-4} to 10^{-3}. Since the main purpose of this paper is to show that RCIE is able to eliminate random walk in integration, we correct the bias in the estimated integral so that the effectiveness of the method against trapezoidal integration is clear in the plots.

Example 4.1: Integrating a single harmonic signal. Let $y(t) = \sin(\omega t)$ be the signal to be integrated, so that the exact integral is $Y(t) = 1/\omega - 1/\omega\cos(\omega t)$. Let $T_{\rm s} = 10^{-3}$ sec/step. Then the measured output is $y_k = \sin(10^{-3}\omega k) + v_k$. Let $n_{\rm e} = 2$, $n_{\rm f} = 1$, $R_\theta = 10^{-6}I_6, R_z = 1$, and $V_1 = 10^{-2}I_2$. The value of V_2 is chosen to set the desired signal-to-noise ratio (SNR).

For $\omega = 10$, Figures 1(a) and 2(a) compare RCIE integration and trapezoidal integration with exact integration for SNRs of 80 dB and 20 dB, respectively. For $\omega = 10$, Figures 1(b) and 2(b) compare the error in RCIE integration with the error in trapezoidal integration for SNRs of 80 dB and 20 dB, respectively. These figures show that trapezoidal integration exhibits a diverging random walk, whereas RCIE integration is free from random walk. To provide a quantitative comparison, the logarithm of the normalized root-mean-square errors (RMSE) in estimating the integral for SNRs ranging

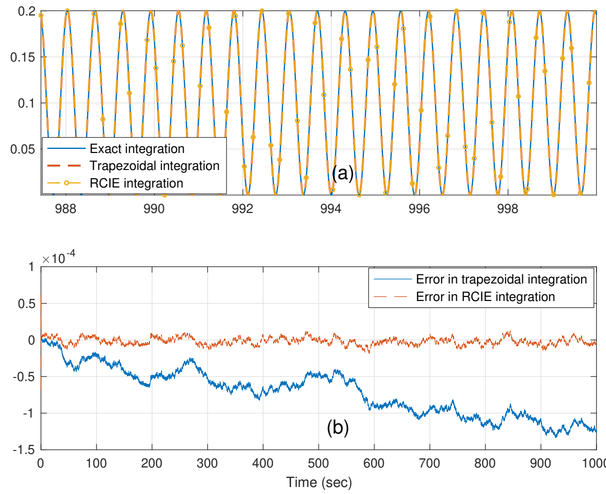

Fig. 1. *Integration of $y(t) = \sin(10t)$ in the presence of* 80 *dB noise.* (a) compares RCIE integration and trapezoidal integration with exact integration. (b) compares the error in RCIE integration with the error in trapezoidal integration. Note that trapezoidal integration exhibits a diverging random walk, whereas RCIE integration is free from random walk.

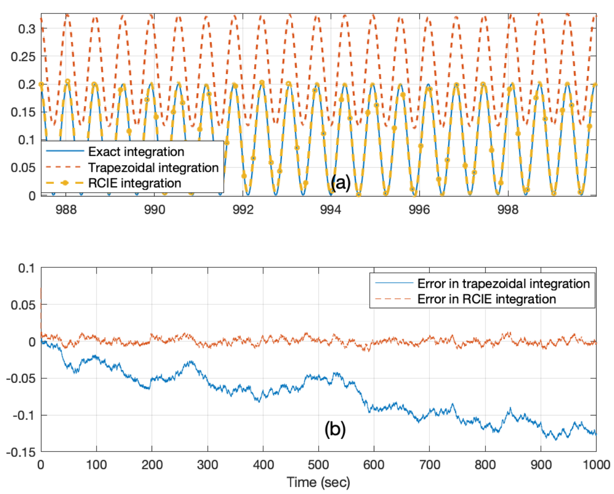

Fig. 2. *Integrating $y(t) = \sin(10t)$ in the presence of* 20 *dB noise.* (a) compares RCIE integration and trapezoidal integration with exact integration. (b) compares the error in RCIE integration with the error in trapezoidal integration. Note that trapezoidal integration exhibits a diverging random walk, whereas RCIE integration is free from random walk.

from 20 dB to 60 dB are plotted in Figures 3, 4, and 5 for $\omega = 1$, $\omega = 10$, and $\omega = 100$ respectively.

Example 4.2: Integrating the sum of two harmonic signals. Let $y(t) = \sin(\omega_1 t) + \sin(\omega_2 t)$ be the signal to be integrated, so that the exact integral is $Y(t) = 1/\omega_1 - 1/\omega_1\cos(\omega t) + 1/\omega_2 - 1/\omega_2\cos(\omega t)$. Let $T_{\rm s} = 10^{-3}$ sec/step. Then the measured output is $y_k = \sin(10^{-3}\omega_1 k) + \sin(10^{-3}\omega_2 k) + v_k$. Let $n_{\rm e} = 3$, $n_{\rm f} = 1$, $R_\theta = 10^{-6}I_6, R_z = 1$, $V_1 = 10^{-2}I_2$. The value of V_2 is chosen to set the desired signal-to-noise ratio (SNR).

For $\omega_1 = 10$ and $\omega_2 = 20$, Figure 6(a) compares RCIE

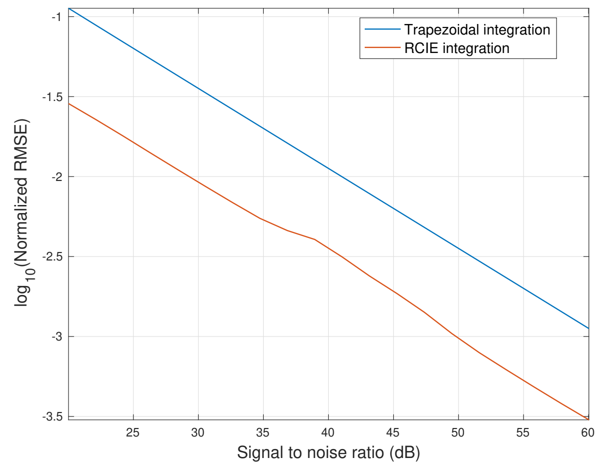

Fig. 3. Logarithm of the normalized RMSE in estimating the integral of $y(t) = \sin(t)$ after 5000 sec versus SNR. RCIE performs better than trapezoidal integration at all SNRs.

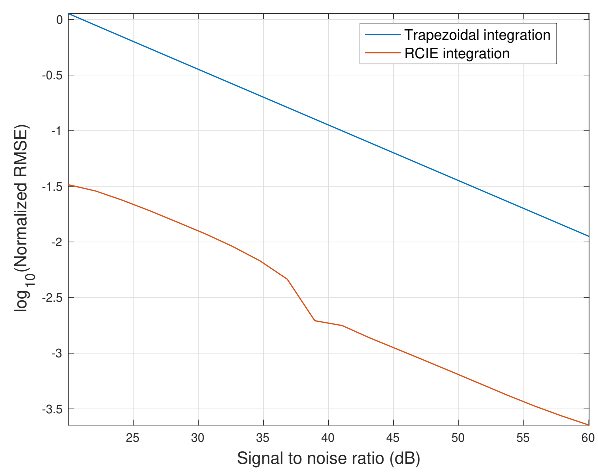

Fig. 4. Logarithm of the normalized RMSE in estimating the integral of $y(t) = \sin(10t)$ after 5000 sec versus SNR. RCIE performs better than trapezoidal integration at all SNRs.

integration and trapezoidal integration with exact integration for an SNR of 20 dB, and Figure 6(b) compares the error in RCIE integration with the error in trapezoidal integration. These figures show that trapezoidal integration exhibits a diverging random walk, whereas RCIE integration is free from random walk. To provide a quantitative comparison, the normalized RMSEs in estimating the integral for SNRs ranging from 20 dB to 60 dB are plotted in Figure 7.

V. CONCLUSIONS

This paper introduced a novel technique for eliminating random walk in the numerical integration of sensor data. This technique is based on the application of retrospective cost input estimation (RCIE), which is an adaptive method for input estimation, to a one-step delayed differentiator. Numerical examples were presented to show the effectiveness of the proposed method. Future research will focus on more complex signals, experimental data, and improving the performance at lower frequencies. Future research will also focus on the ability of RCIE to accurately double-integrate signals. This ability would enable the development of inertial navigation algorithms that are free of random-walk divergence and thus provide significantly improved performance.

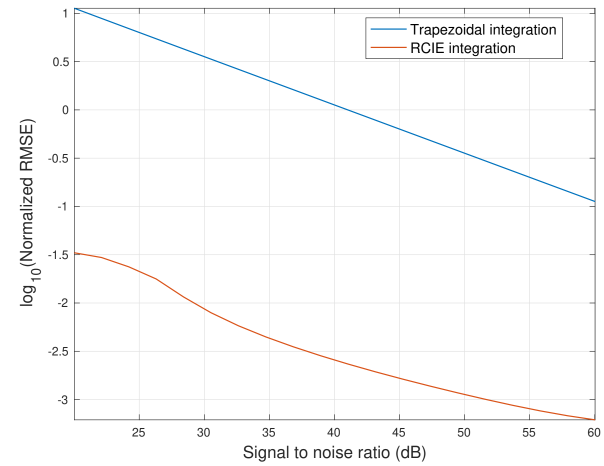

Fig. 5. Logarithm of the normalized RMSE in estimating the integral of $y(t) = \sin(100t)$ after 5000 sec versus SNR. RCIE performs better than trapezoidal integration at all SNRs.

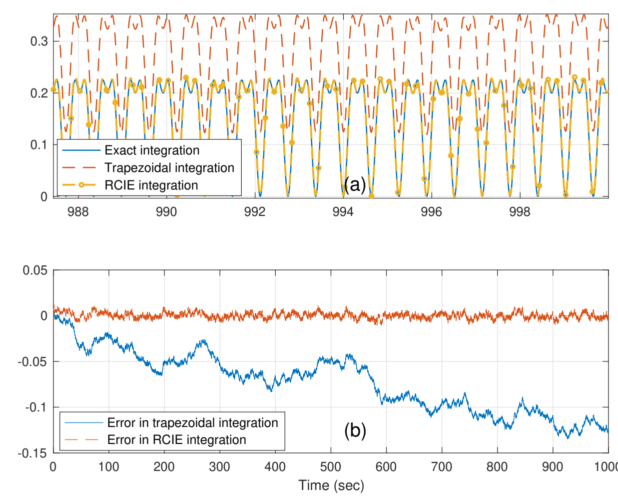

Fig. 6. *Integrating* $y(t) = \sin(10t) + \sin(20t)$ *in the presence of* 20 *dB noise.* (a) compares RCIE integration and trapezoidal integration with exact integration. (b) compares the error in RCIE integration with the error in trapezoidal integration. Note that trapezoidal integration exhibits a diverging random walk, whereas RCIE integration is free from random walk.

ACKNOWLEDGMENTS

This research was supported by NSF under grant CMMI 2031333 and by the Office of Naval Research under grant N00014-18-1-2211 of the BRC Program. We thank the reviewers for helpful comments.

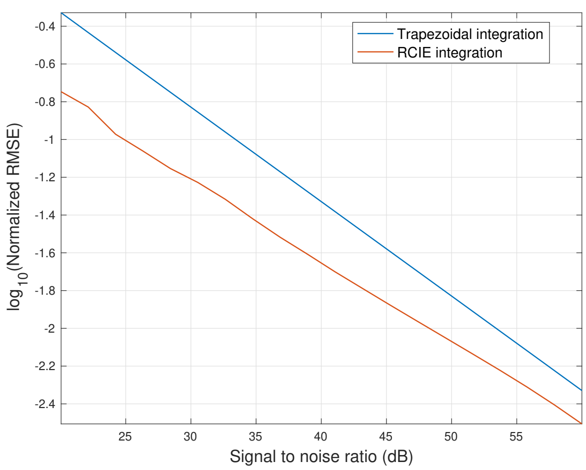

Fig. 7. Logarithm of the normalized RMSE in estimating the integral of $y(t) = \sin(10t) + \sin(20t)$ after 5000 sec versus SNR. RCIE performs better than trapezoidal integration at all SNRs.

REFERENCES

[1] F. E. Burk, *A Garden of Integrals*. MAA, 2007.

[2] P. J. Davis and P. Rabinowitz, *Methods of Numerical Integration*. Dover, second ed., 2007.

[3] J. C. Butcher, *Numerical Methods for Ordinary Differential Equations*. Wiley, third ed., 2016.

[4] E. Hairer, C. Lubich, and G. Wanner, *Geometric Numerical Integration*. Springer, 2002.

[5] D. S. Bernstein, "Sensor Performance Specifications," *IEEE Contr. Sys. Mag.*, vol. 21, pp. 9–18, August 2001.

[6] A. Chatfield, *Fundamentals of High Accuracy Inertial Navigation*. AIAA, 1997.

[7] S. Merhav, *Aerospace Sensor Systems and Applications*. Springer, 1998.

[8] C. Jekeli, *Inertial Navigation Systems with Geodetic Applications*. De Gruyter, 2000.

[9] J. A. Farrell, *Aided Navigation: GPS with High Rate Sensors*. McGraw-Hill, 2008.

[10] A. Lawrence, *Modern Inertial Technology: Navigation, Guidance, and Control*. Springer, 2012.

[11] P. D. Groves, *Principles of GNSS, Inertial, and Multisensor Integrated Navigation Systems*. Artech House, second ed., 2013.

[12] P. T. Kabamba and A. R. Girard, *Fundamental of Aerospace Navigation and Guidance*. Cambridge, 2014.

[13] M. S. Grewel, A. P. Andrews, and C. G. Bartone, *Global Navigation Satellite Systems, Inertial Navigation, and Integration*. Wiley, fourth ed., 2020.

[14] A. Goel, S. A. U. Islam, A. Ansari, O. Kouba, and D. S. Bernstein, "An Introduction to Inertial Navigation from the Perspective of State Estimation," *IEEE Contr. Sys. Mag.*, vol. 41, pp. 104–129, Oct. 2021.

[15] Y. K. Thong, M. S. Woolfson, J. A. Crowe, B. R. Hayes-Gill, and R. Challis, "Dependence of Inertial Measurements of Distance on Accelerometer Noise," *Meas. Sci. Tech.*, vol. 13, pp. 1163–1172, 2002.

[16] Y. K. Thong, M. S. Woolfson, J. A. Crowe, B. R. Hayes-Gill, and D. A. Jones, "Numerical Double Integration of Acceleration Measurements in Noise," *Measurement*, vol. 36, no. 1, pp. 73–92, 2004.

[17] V. Cviklovic, D. Hruby, M. Olejar, and O. Lukac, "Comparison of Numerical Integration Methods in Strapdown Inertial Navigation Algorithm," *Res. Agr. Eng.*, vol. 57, pp. S30–S34, 2011.

[18] S. Thenozhi, W. Yu, and R. Garrido, "A Novel Numerical Integrator for Velocity and Position Estimation," *Trans. Inst. Meas. Contr.*, vol. 35, no. 6, pp. 824–833, 2013.

[19] Y.-Z. Yang and D.-X. Jiang, "Numerical Integration and Complex Trend Term Elimination of Acceleration Signal in Fault Diagnosis," in *Proc. Int. Power, Elect. Mat. Eng. Conf.*, pp. 495–500, 2015.

[20] X. Kong, W. Yang, and B. Li, "Application of Stabilized Numerical Integration Method in Acceleration Sensor Data Processing," *IEEE Sensors J.*, vol. 21, no. 6, pp. 8194–8203, 2021.

[21] M. Hou and R. J. Patton, "Input Observability and Input Reconstruction," *Automatica*, vol. 34, no. 6, pp. 789–794, 1998.

[22] M. Corless and J. Tu, "State and Input Estimation for a Class of Uncertain Systems," *Automatica*, vol. 34, no. 6, pp. 757–764, 1998.

[23] T. Floquet and J. P. Barbot, "State and Unknown Input Estimation for Linear Discrete-Time Systems," *Automatica*, vol. 42, pp. 1883–1889, 2006.

[24] S. Gillijns and B. De Moor, "Unbiased Minimum-Variance Input and State Estimation for Linear Discrete-Time Systems," *Automatica*, vol. 43, no. 1, pp. 111–116, 2007.

[25] R. Orjuela, B. Marx, J. Ragot, and D. Maquin, "On the Simultaneous State and Unknown Input Estimation of Complex Systems via a Multiple Model Strategy," *IET Contr. Theory Appl.*, vol. 3, no. 7, pp. 877–890, 2009.

[26] H. Fang, R. A. de Callafon, and J. Cortes, "Simultaneous Input and State Estimation for Nonlinear Systems with Applications to Flow Field Estimation," *Automatica*, vol. 49, no. 9, pp. 2805–2812, 2013.

[27] S. Z. Yong, M. Zhu, and E. Frazzoli, "A Unified Filter for Simultaneous Input and State Estimation of Linear Discrete-Time Stochastic Systems," *Automatica*, vol. 63, pp. 321–329, 2016.

[28] P. Lu, E.-J. van Kampen, C. C. de Visser, and Q. Chu, "Framework for State and Unknown Input Estimation of Linear Time-Varying Systems," *Automatica*, vol. 73, pp. 145–154, 2016.

[29] C.-S. Hsieh, "Unbiased Minimum-Variance Input and State Estimation for Systems with Unknown Inputs: A System Reformation Approach," *Automatica*, vol. 84, pp. 236–240, 2017.

[30] S. Sanjeevini and D. S. Bernstein, "Minimal-Delay FIR Delayed Left Inverses for Systems with Zero Nonzero Zeros," *Sys. Contr. Lett.*, vol. 133, p. 104552, 2019.

[31] E. Naderi and K. Khorasani, "Unbiased Inversion-Based Fault Estimation of Systems with Non-Minimum Phase Fault-to-Output Dynamics," *IET Contr. Th. & Appl.*, vol. 13, no. 11, pp. 1629–1638, 2019.

[32] B. Alenezi, M. Zhang, S. Hui, and S. H. Żak, "Simultaneous Estimation of the State, Unknown Input, and Output Disturbance in Discrete-Time Linear Systems," *IEEE Trans. Autom. Contr.*, vol. 66, no. 12, pp. 6115–6122, 2021.

[33] G. Gakis and M. C. Smith, "A Deterministic Least Squares Approach for Simultaneous Input and State Estimation," *IEEE Trans. Autom. Contr.*, 2022.

[34] P.-C. Tuan and W.-T. Hou, "Adaptive Robust Weighting Input Estimation Method for the 1-D Inverse Heat Conduction Problem," *Numerical Heat Transfer, Part B*, vol. 34, no. 4, pp. 439–456, 1998.

[35] H.-M. Wang, T.-C. Chen, P.-C. Tuan, and S.-G. Den, "Adaptive-Weighting Input-Estimation Approach to Nonlinear Inverse Heat-Conduction Problems," *Journal of Thermophysics and Heat Transfer*, vol. 19, no. 2, pp. 209–216, 2005.

[36] T. D. Grifith, V. P. Gehlot, and M. J. Balas, "Adaptive Estimation of Unknown Inputs with Weakly Nonlinear Dynamics," in *Proc. Amer. Contr. Conf.*, pp. 5043–5049, 2022.

[37] A. Ansari and D. S. Bernstein, "Adaptive Input Estimation for Nonminimum-Phase Discrete-Time Systems," in *IEEE Conference on Decision and Control*, pp. 1159–1164, 2016.

[38] L. Han, Z. Ren, and D. S. Bernstein, "Maneuvering Target Tracking Using Retrospective-Cost Input Estimation," *IEEE Transactions on Aerospace and Electronic Systems*, vol. 52, no. 5, pp. 2495–2503, 2016.

[39] A. Ansari and D. S. Bernstein, "Input Estimation for Nonminimum-Phase Systems With Application to Acceleration Estimation for a Maneuvering Vehicle," *IEEE Trans. Contr. Syst. Tech.*, vol. 27, no. 4, pp. 1596–1607, 2019.

[40] S. Verma, S. Sanjeevini, E. D. Sumer, A. Girard, and D. S. Bernstein, "On the Accuracy of Numerical Differentiation Using High-Gain Observers and Adaptive Input Estimation," in *Proc. Amer. Contr. Conf.*, pp. 4068–4073, June 2022.

[41] S. Sanjeevini and D. S. Bernstein, "Decomposition of the Retrospective Performance Variable in Adaptive Input Estimation," in *Proc. Amer. Contr. Conf.*, pp. 242–247, June 2022.